InP-based lattice-matched InGaAsP and strain-compensated InGaAs / InGaAs quantum well cells for thermophotovoltaic applications

Carsten Rohr, Paul Abbott, Ian Ballard, James P. Connolly, and Keith W. J. BarnhamMassimo MazzerChris ButtonLucia NasiGeoff Hill and John S. RobertsGraham ClarkeRavin Ginige

Citation: Journal of Applied Physics **100**, 114510 (2006); doi: 10.1063/1.2398466

View online: http://dx.doi.org/10.1063/1.2398466

View Table of Contents: http://aip.scitation.org/toc/jap/100/11

Published by the American Institute of Physics

InP-based lattice-matched InGaAsP and strain-compensated InGaAs/InGaAs quantum well cells for thermophotovoltaic applications

Carsten Rohr, Paul Abbott, Ian Ballard, James P. Connolly, and Keith W. J. Barnham[a)]
Experimental Solid State Physics, Blackett Laboratory, Imperial College London, London SW7 2BW, United Kingdom

Massimo Mazzer
CNR-IMM, Sezione di Lecce, Via Arnesano, 73100 Lecce, Italy

Chris Button
Bookham, Caswell, Towcester, Northants NN12 8EQ, United Kingdom

Lucia Nasi
CNR-IMEM, Sezione di Parma, Parco Area delle Scienze 37/A, 43010 Fontanini, Parma, Italy

Geoff Hill and John S. Roberts
EPSRC National Cèntre for III-V Technologies, Sheffield S1 3JD, United Kingdom

Graham Clarke
IQE Europe Ltd., Cardiff CF3 0EG, United Kingdom

Ravin Ginige
Tyndall National Institute, Cork, Ireland

(Received 2 June 2006; accepted 16 September 2006; published online 8 December 2006)

Quantum well cells (QWCs) for thermophotovoltaic (TPV) applications are demonstrated in the InGaAsP material system lattice matched to the InP substrate and strain-compensated InGaAs/InGaAs QWCs also on InP substrates. We show that lattice-matched InGaAsP QWCs are very well suited for TPV applications such as with erbia selective emitters. QWCs with the same effective band gap as a bulk control cell show a better voltage performance in both wide and erbialike emission. We demonstrate a QWC with enhanced efficiency in a narrow-band spectrum compared to a bulk heterostructure control cell with the same absorption edge. A major advantage of QWCs is that the band gap can be engineered by changing the well thickness and varying the composition to the illuminating spectrum. This is relatively straightforward in the lattice-matched InGaAsP system. This approach can be extended to longer wavelengths by using strain-compensation techniques, achieving band gaps as low as 0.62 eV that cannot be achieved with lattice-matched bulk material. We show that strain-compensated QWCs have voltage performances that are at least as good as, if not better than, expected from bulk control cells. [DOI: 10.1063/1.2398466]

I. INTRODUCTION

In a quantum well cell (QWC) nanometer thick layers of low band gap material are introduced into the intrinsic region of a *p-i-n* diode in order to increase the absorption of the photovoltaic (PV) cell.[1] The absorption threshold, or effective band gap, can be tuned by varying the material composition of these quantum wells (QWs) and, because of the quantum confinement, by changing their thickness. For cells based on the InP substrate, a wide range of lattice-matched materials is available, $In_{1-x}Ga_xAs_yP_{1-y}$ with $x \sim 0.47y$, where the band gap can be varied downwards from 1.35 eV (absorption edge 0.9 μm) to 0.73 eV (absorption edge 1.7 μm), with $In_{0.53}Ga_{0.47}As$ having the lowest possible band gap of this lattice-matched material system.

The absorption can be extended if the QWs are strained to the substrate. But only a few QWs can be grown before dislocations form and the device quality deteriorates due to nonradiative recombination.[2] This restriction can be overcome by strain compensating QWs and barriers. In principle, an unlimited number of periods can be grown without strain relaxation if the stress is minimized as discussed in Refs. 3 and 4.

In thermophotovoltaics (TPV),[5,6] heat radiation is converted into electricity, as opposed to sunlight in a conventional PV cell. The source is at a lower temperature for TPV applications, typically around 1500–2000 K, as opposed to the 5800 K of the sun. The peak of a lower temperature blackbody spectrum is at a longer wavelength, hence lower band-gap semiconductors offer a better spectral match. It is also possible to shape the illuminating spectrum, for example, by introducing selective emitters between the source and the cells to obtain a narrow-band spectrum,[7] which increases the photovoltaic conversion efficiency when matched to the band gap of the cell. Such selective emitters are often

[a)]Author to whom correspondence should be addressed; electronic mail: k.barnham@imperial.ac.uk

TABLE I. Sample description of a typical lattice-matched quaternary QWC MR1178. $Q1.1$ and $Q1.6$ represent the quaternary InGaAsP material with a bulk absorption edge of about 1.1 and 1.6 μm, respectively.

	Layer	Repeats	Thickness (Å)	Material	Doping	Concentration (cm^{-3})
Lattice-matched MQW	Cap/contact	1	1000	InGaAs	p	3×10^{18}
	Emitter	1	1500	InP	p	8×10^{17}
	Spacer	1	2500	InP	i	
	Barrier	60	70	$Q1.1$	i	
	Well	60	100	$Q1.6$	i	
	Barrier	1	70	$Q1.1$	i	
	Base/buffer	1	5000	InP	n	3×10^{18}

based on rare-earth elements, such as erbium, thulium, or holmium with peak emission of about 1.5, 1.8, and 2.1 μm, respectively.[7]

In this paper we study and analyze lattice-matched InGaAsP QWCs suitable for an erbium-based emitter (Sec. III A), and strain-compensated InGaAs/InGaAs QWCs for a thulium-based emitter (Sec. III B). A more general review of QWCs for TPV applications is given in Ref. 8.

II. EXPERIMENT

The lattice-matched InGaAsP devices were grown on InP substrates by metal-organic vapor-phase epitaxy (MOVPE) at the EPSRC National Centre for III-V Technologies in Sheffield, United Kingdom. A typical sample with a multi-quantum-well (MQW) region is given in Table I. The layers were grown on epiready (100) InP substrates, n type with sulphur, and usually with a misorientation of 0.35° off to (110). The p and n type layers are InP, whereas the ~1 μm wide intrinsic region is made of the quaternary $Q1.1$ (where the Q value indicates the bulk absorption edge in microns) with a composition of $y\sim0.36$ resulting in a bulk absorption edge of 1.1–1.15 μm. Incorporated into this i region are 60 QWs of 10 nm width made of the quaternary $Q1.6$ with a composition of $y\sim0.86$ equivalent to a bulk absorption edge of about 1.6 μm. Due to the confinement the effective absorption edge is closer to 1.5 μm. A 0.2 μm wide spacer region is introduced between the i and p region to reduce Zn dopant diffusion into the QWs.[9] The top InGaAs cap layer serves for contacting the device. When an antireflection (AR) coating is applied, the cap is etched off in the optical window.

Some strain-compensated samples were also grown in Sheffield (prefix "MR"), but most were grown by IQE Ltd., Cardiff, Wales (prefix "E"), also by MOVPE, such as E1055 shown in Table II.

Test devices were processed into 1 mm diameter mesas with a contact ring leaving an optical window of 600 μm diameter. A Keithley 238 source-measurement unit was used for current-voltage (I-V) measurements in the dark and under illumination. The temperature of the sample, which was kept constant at 25 °C using a Peltier plate, was monitored with a Keithley 142 digital multimeter and a platinum resistance thermometer. An Oriel quartz halogen tungsten lamp was used as light source with a stabilized dc power supply and a fiber lead, approximating a 3000 K blackbody spectrum. A filter which transmitted a narrow-band spectrum resembling erbia emission (see Fig. 1) could also be added to the fiber lead. The optical power density was set to a constant level using a calibration cell.

The quantum efficiency (QE) was measured using a Bentham M300 0.3 m monochromator with a 100 W tungsten lamp as a light source and a Bentham current stabilized filament lamp power supply 505. The photocurrent is measured with a lock-in technique using a Stanford Research Systems SR510 lock-in amplifier with a Bentham 218 variable frequency optical chopper at a frequency of about 187 Hz. Two such setups were used, one for the visible range (400–1100 nm) with a calibrated Si detector, and another one for the infrared range (850–2000 nm) with calibrated InGaAs (850–1650 nm) and extended InGaAs (1300–2000 nm) detectors from Hamamatsu.

TABLE II. Sample description of strain-compensated QWC E1055.

	Layer	Repeats	Thickness (Å)	Material	Doping	Concentration (cm^{-3})
Strain-compensated MQW	Cap/contact	1	3000	InGaAs	p	1×10^{19}
	Emitter	1	3000	InP	p	2×10^{18}
	Spacer	1	2000	InP	i	
	Barrier	40	89	$In_{0.45}Ga_{0.55}As$	i	
	Well	40	80	$In_{0.74}Ga_{0.26}As$	i	
	Barrier	40	89	$In_{0.45}Ga_{0.55}As$	i	
	Buffer	1	200	InP	i	
	Base	1	5000	InP	n	1×10^{18}

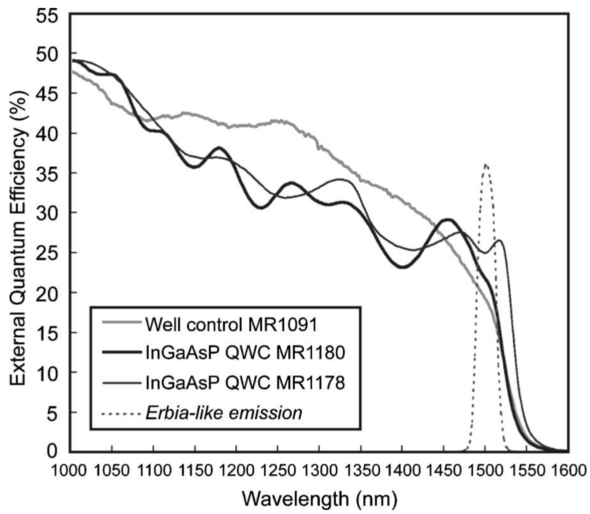

FIG. 1. External quantum efficiency at zero bias of QWCs MR1180 and MR1178, compared with well control MR1091 (all non-AR). The position of an erbia peak is also indicated (arbitrary intensity).

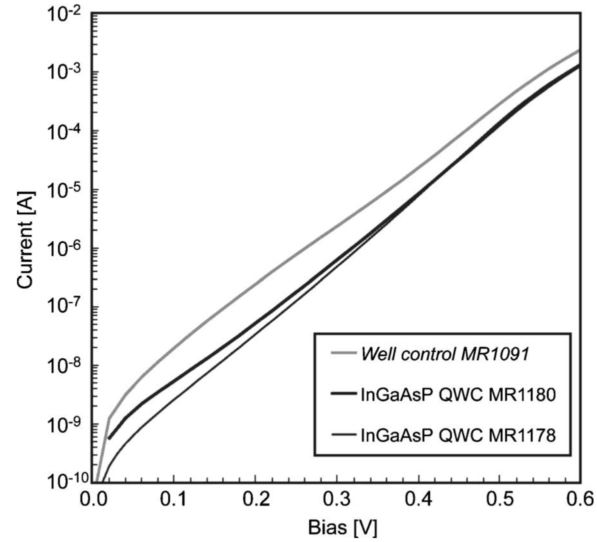

FIG. 2. Dark current densities of QWCs MR1180 and MR1176, compared with well control MR1091.

III. RESULTS

A. Lattice-matched InGaAsP QWCs

Several lattice-matched InGaAsP QWCs were grown similar to MR1178 (see Table I) and a nominally identical sample MR1180 which had an additional etch-stop layer between the base and the substrate for front contacting. For comparison, control samples without QWs but otherwise the same as in Table I (i.e., with the same total *i*-region width) were grown: a barrier control MR1088, where the whole QW region is replaced by the barrier material *Q*1.1; and a well control MR1091 where the whole QW region is replaced by a quaternary material composition so that the effective absorption edge is the same as in the QWC (i.e., material with a slightly wider band gap than *Q*1.6 to compensate for the confinement in the QWs). Hence samples MR1088 and MR1091 are double heterostructures. They have the same thickness of InP *i*-region spacer as the QWCs in Table I but the QW system is replaced by lower band gap, bulk intrinsic material with band gap similar to either the barrier or the well. The thickness of the bulk material is equal to the 1.027 μm of well plus barrier material in the QWC.

As one can see in Fig. 1, samples MR1091 and MR1180 have exactly the same absorption edge, while MR1178 extends somewhat further. These samples are very well suited for TPV applications with erbium-based selective emitters which have a peak at about 1500 nm (also indicated in Fig. 1). Note that Fig. 1 also shows that a multi-QW system of 60 wells and barriers has comparable absorption to a bulk semiconductor with the same effective absorption edge and a thickness equal to the total of wells and barrier.

One would expect the voltage performance to be determined by the band gap of the QW material. The most challenging situation is to compare samples with the same effective threshold, as in this set of samples. Although the absorption threshold is identical for MR1091 and MR1180 (see Fig. 1), the dark current density of the QWC is significantly lower than that of the well control as shown in Fig. 2. The QWC MR1178 shows even better material quality having a similarly low dark current as QWC MR1180 while the absorption is extended to slightly longer wavelengths.

Barnham *et al.* have demonstrated a voltage enhancement of QWCs compared to their bulk control cells in the lattice-matched material systems AlGaAs/GaAs, GaInP/GaAs, and InP/InGaAs.[10] However, in those cases the control cells were made of the same material as the QWs, which means that the bulk control cells have slightly lower effective band gaps due to the confinement in the QWs. Here we demonstrate that a QWC with the same *effective absorption edge* as a bulk control (Fig. 1) shows a lower dark current (Fig. 2). We will show later that this leads to voltage enhancement in a 3000 K spectrum (Fig. 4) and in erbialike emission (Fig. 5).

Figure 2 provides further evidence that QWCs have a better dark current than expected from their absorption threshold.[10] In Fig. 3 this is confirmed for a number of samples in the material system $In_{1-x}Ga_xAs_yP_{1-y}$ on InP. One might expect the dark current (for example, at a typical operating point such as a bias of 0.4 V) of the QWCs to lie on a line connecting the two homogenous bulk controls InP and InGaAs (Fig. 3), including an InGaAs monolithic intercon-

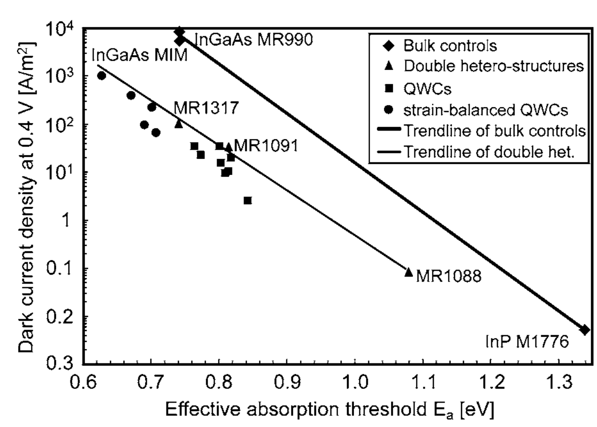

FIG. 3. Dark current density at a fixed bias of 0.4 V vs absorption threshold. The bulk and double-heterostructure cells have been individually identified.

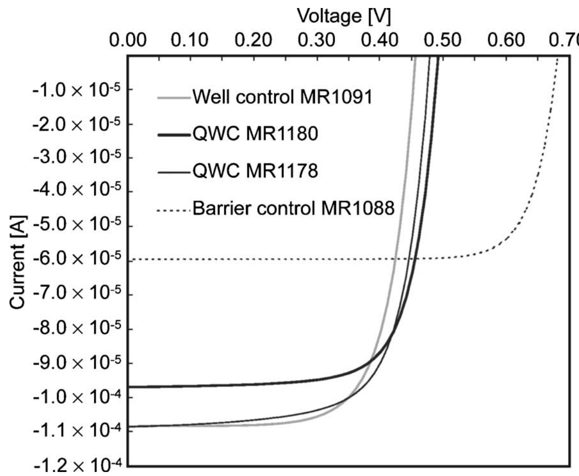

FIG. 4. *I-V* curves of QWCs MR1180 and MR1178, well control MR1091, and barrier control MR1088 under 3000 K blackbody illumination.

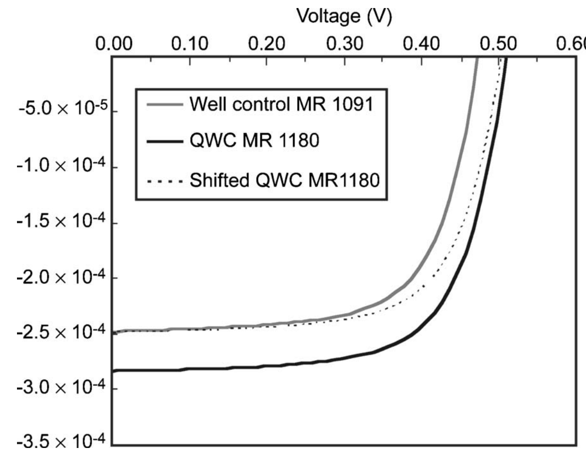

FIG. 5. Measured light *I-V* characteristics of MR1091 compared to MR1180 under 1500 nm narrow-band illumination. Also shown is MR1180 shifted down to the same short-circuit current as MR1091.

nected module (MIM).[11] However, all the QWCs have a much lower dark current than that by about two orders of magnitude. The dark current depends to some degree on the number of QWs, particularly for a small number of QWs, but here we consider large numbers of QWs as all the lattice-matched QWCs have 60 QWs. Also included in Fig. 3 are double heterostructures such as MR1091 and MR1088 which are described above.

Although double heterostructures have a much lower dark current than the homogenous controls, their dark current is not as low as most QWCs. Figures 2 and 3 show that InGaAsP QWCs have reduced dark currents and reduced recombination and hence a clear advantage over homogenous bulk control cells and even over double heterostructures. We will now investigate whether this reduced recombination translates into an improved voltage performance and improved efficiency under illumination.

The *I-V* characteristics under illumination from the 3000 K blackbody source are shown for some of the cells in Fig. 4. Although the absorption thresholds of MR1091 and MR1180 are identical, the well control MR1091 has a slightly higher short-circuit current (I_{sc}) than the QWC MR1180 because it has a slightly higher QE in the range of 1100–1450 nm (see Fig. 1) which gives rise to a considerable contribution under the broad illuminating spectrum. Even though I_{sc} is smaller for MR1180 than for MR1091, the V_{oc} is significantly higher for MR1180. It shows that the reduced dark current and reduced recombination lead to a higher V_{oc} under illumination.

TABLE III. Light *I-V* characteristics under 3000 K blackbody illumination. All samples are 1 mm diameter mesas with 600 μm diameter optical window and the cap is left on with no AR coating.

Sample	V_{oc} (V)	I_{sc} (μA)	Fill factor	Power output (μW)
QWC MR1178	0.477	109	0.699	36
Well control MR1091	0.455	108	0.712	35
QWC MR1180	0.491	97.0	0.727	35
Barrier control MR1088	0.681	59.3	0.803	32

The QWC MR1178 shows an improvement in performance over both the barrier control (MR1088) and the well control (MR1091) even under this broad illuminating spectrum (Table III). This is mainly due to an enhancement in V_{oc} compared to the well control, and a much better I_{sc} compared to the barrier control. However, the fill factor of MR1178 is slightly inferior compared to both controls. It should be noted that these numbers are for comparison relative to each other.

The light *I-V*'s of the cells was then measured when illuminated through a filter thus simulating erbialike emission. It can be seen from Fig. 1 that the QWC MR1180 has a higher absorption than the well control MR 1091 just above threshold even though they have the same absorption edge. Hence, a combination of absorbing QWs and transparent barriers with the same total thickness as bulk material in a double heterostructure with the same absorption edge results in higher absorption just above threshold. It is well known that this is due to the stronger excitonic absorption in a QW compared to the bulk due to quantum confinement. The excitonic signal in MR1180 is masked in Fig. 1 due to optical cavity effects. The exciton is clearer in MR1178.

It can be seen from Fig. 5 and Table IV that the QWC MR1180 has a higher V_{oc} and higher efficiency under erbialike illumination than the double heterostructure control MR1091 with the same absorption edge. Part of this advantage comes from the increased absorption just above threshold observed in Fig. 1. In Fig. 5 and Table IV we therefore also show the *I-V* when the I_{sc} of the QWC cell is scaled

TABLE IV. Light *I-V* characteristics under 1500 nm narrow-band illumination. All samples are 1 mm diameter mesas with 600 μm diameter optical window and the cap is left on with no AR coating.

Sample	V_{oc} (V)	I_{sc} (μA)	Fill factor	Power output (μW)
QWC MR1180	0.513	285.8	0.67	99.2
QWC scale I_{sc}	0.503	250.4	0.67	84.8
Well control MR1091	0.476	250.4	0.68	79.6

down to be the same as the well control. It can be seen that both the V_{oc} and the efficiency of the QWC are still higher than the well control.

We have therefore demonstrated that the improved dark current in a QWC compared with a bulk double-heterostructure cell with the same absorption edge results in an improved V_{oc} in both broad and narrow-band illumination, and an improved efficiency in a narrow-band spectrum.

The absolute performance of these cells can be much improved by employing an appropriate grid design and optimizing the front layers (e.g., etching off the cap layer in the optical window) and applying AR coats. In a TPV system, the illuminating spectrum and the spectral response of the cells should be matched to increase the efficiency. The system efficiency can be further improved, for example, by employing a mirror at the back of the device to reflect photons which have not been absorbed such as low-energy photons back to the source. Such a mirror is particularly advantageous for QWCs because the QE of the QWs is increased as photons have the chance of a second pass through the QWs.

B. Strain-balanced InGaAs/InGaAs QWCs

For TPV applications, there is increasing interest in longer wavelengths selective emitters, for example, based on thulium and holmium, in order to match lower temperature blackbody spectra and hence achieving higher system efficiencies compared to erbia and ytterbia.[7,12] Burning fossil fuels at lower temperature at around 1500 K reduces NO_x emissions.

For such applications low band-gap material is required to match the long wavelength selective emitter. However, appropriate and inexpensive substrates of the required lattice constant and band gap are not readily available, so the lower band-gap material is often strained. If the material exceeds a critical thickness, dislocations are introduced which increase nonradiative recombination. In MQW systems one can avoid this strain relaxation by strain compensating the layers; alternating wells and barriers have bigger and smaller lattice constants, but each period is lattice matched to the substrate.

Differences in elastic constants may need to be taken into account to minimize the stress.[3,4] Using this method, it is possible to obtain smaller effective band gaps in the quantum wells than the lattice-matched material, and hence extend the absorption towards longer wavelengths without introducing excess dislocations. As long as each individual layer remains below the critical thickness, in principle an unlimited number of periods can be grown without introducing any dislocations. However, this technique is limited by the formation of strain-balance defects.[13,14] They are caused by the onset of undulations (wavy growth) which originate in the tensile barrier layers. The maximum number of defect-free periods in an InGaAs/InGaAs strain-compensated MQW is proportional to the inverse of the elastic energy density per unit area stored in each period.[13,15]

Several strain-compensated samples have been grown, and one of these sample (E1055) is described in Table II. This sample has a high indium content of about 74% in the QWs, in order to extend the absorption to about 1.95 μm,[16] but the high In fraction also results in a high misfit of about 1.4%. The barriers, by contrast, were designed to be much wider to reduce the misfit to about −0.47%. This way undulations and strain-balance defects could be avoided as is evident from the transmission electron micrograph in Fig. 6.

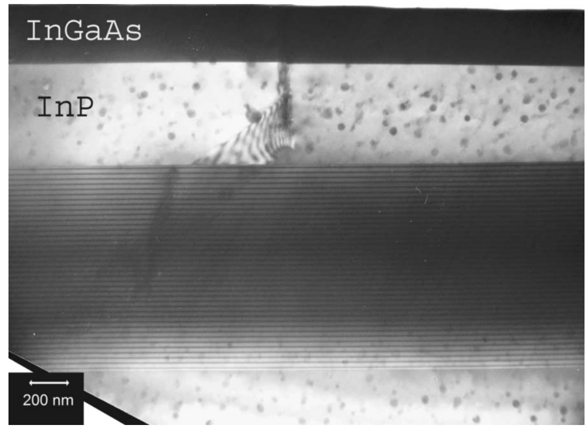

FIG. 6. Cross-sectional transmission electron micrograph of strain-compensated QWC E1055 (see Table II).

Several strain-compensated QWCs are also included in Fig. 3 showing that even in the case of strain compensation the dark current density is lower than expected from the absorption threshold. The line of expected performance as indicated in Fig. 3 is extrapolated from the results of lattice-matched bulk devices, as for these absorption thresholds no lattice-matched bulk material is available. This shows that with strain compensation one can extend the absorption and at the same time obtain excellent results for strain-compensated QWCs, having similar or better voltage performance than expected based on the trends in the bulk material in Fig. 3.

IV. CONCLUSIONS

We have shown that lattice-matched InGaAsP QWCs are very well suited for TPV applications such as with erbia selective emitters. We have demonstrated that QWCs show a better voltage performance in both wide-band and narrow-band spectra and higher efficiency in erbialike emission, than a bulk heterostructure with the same absorption edge. Hence a QWC can lower the dark current and enhance the band-edge absorption, the V_{oc}, and the efficiency compared to a bulk heterostructure control cell with the same effective threshold. The higher absorption and efficiency in narrow-band spectra would be useful in power-over fiber applications as well as TPV. A major advantage of QWCs is that the band gap can be engineered by changing the well thickness and varying the composition to fit the illuminating spectrum. This is relatively straightforward in the lattice-matched InGaAsP system, but it can be extended to longer wavelengths by using strain-compensation techniques, achieving band gaps that cannot be achieved with lattice-matched bulk material. We have shown that even such Strain-compensated QWCs have voltage performances that are at least as good as, if not better than expected. Strain-compensated QWCs are promising candidates for TPV applications, for example, with thulia and/or holmia selective emitters.

ACKNOWLEDGMENTS

This research benefited from the financial support by the UK Engineering and Physical Science Research Council (Grant No. GR/L50471) and the European Commission (Grant No. ERK6-CT-1999-00019).

[1]K. W. J. Barnham and G. Duggan, J. Appl. Phys. **67**, 3490 (1990).
[2]N. Ekins-Daukes, K. Barnham, J. Connolly, J. Roberts, J. Clark, G. Hill, and M. Mazzer, Appl. Phys. Lett. **75**, 4195 (1999).
[3]N. Ekins-Daukes, K. Kawaguchi, and J. Zhang, Cryst. Growth Des. **2**, 287 (2002).
[4]C. Rohr, J. P. Connolly, N. Ekins-Daukes, P. Abbott, I. Ballard, K. W. Barnham, M. Mazzer, and C. Button, Physica E (Amsterdam) **14**, 158 (2002).
[5]T. J. Coutts, Renewable Sustainable Energy Rev. **3**, 77 (1999), 13
[6]*Special Issue on Thermophotovoltaics*, Semiconductor Science and Technology Vol. 18, edited by K. Bamham, J. Connolly, and C. Rohr (Institute of Physics Publishing, Bristol, 2003).
[7]A. Licciulli, D. Diso, G. Torsello, S. Tundo, A. Maffezzoli, M. Lomascolo, and M. Mazzer, Semicond. Sci. Technol. **18**, S174 (2003).
[8]J. P. Connolly and C. Rohr, Semicond. Sci. Technol. 18, (2003), special issue on thermophotovoltaics, edited by K. Barnham, J. Connolly, and C. Rohr.
[9]A. Zachariou, K. W. J. Barnham, P. Grffin, J. Nelson, C. C. Button, M. Hopkinson, M. Pate, and J. Epler, in *Proceedings of the 25th IEEE PV Specialists Conference* (IEEE, Piscataway, 1996), pp. 113–116.
[10]K. W. J. Barnham *et al.*, J. Appl. Phys. **80**, 1201 (1996).
[11]N. S. Fatemi *et al.*, *Proceedings of the 26th IEEE PV Specialists Conference* (IEEE, Piscataway, 1997), pp. 799–804.
[12]M. Mazzer, A. De Risi, D. Laforgia, K. Barnham, and C. Rohr, in *Proceedings of the Society of Automotive Engineers 2000 World Congress, Michigan, 2000* (Society of Automotive Engineers, Troy, MI, 2000) [SAE Tech. Pap. Ser. **2000-01**, 991 (2000)].
[13]L. Nasi, C. Ferrari, L. Lazzarini, G. Salviati, S. Tundo, M. Mazzer, G. Clarke, and C. Rohr, J. Phys.: Condens. Matter **14**, 13367 (2002).
[14]S. Tundo *et al.*, J. Appl. Phys. **94**, 6341 (2003).
[15]L. Nasi, C. Ferrari, L. Lazzarini, and G. Clarke, J. Appl. Phys. **92**, 7678 (2002).
[16]P. Abbott *et al.*, in *The Fifth Conference on Thermophotovoltaic Generation of Electricity, Rome, Italy, 2002*, edited by T. J. Coutts, G. Guazzoni, and J. Luther (AIP, Woodbury, New York, 2003) [AIP Conf. Proc. **653**, 213 (2002)].